Additional Material: Accelerated Monte Carlo Rendering of Finite-Time Lyapunov Exponents

Irene Baeza Rojo, Markus Gross, and Tobias Günther

1 Single-Scattered Gradient Domain Rendering

As shown in the main paper, the α-weight in Eq. (11) determines a compromise between the estimate of the base image and the estimated gradients. Fig. 1 depicts the screened Poisson reconstruction results for different α values in the ABC [2] flow, an analytic benchmark data set that contains vortex tubes that are separated by FTLE ridge surfaces . The higher α, the less gradient information is used. Lehtinen et al. [3] recommended a default value of $\alpha = 1$, which we used in the paper.

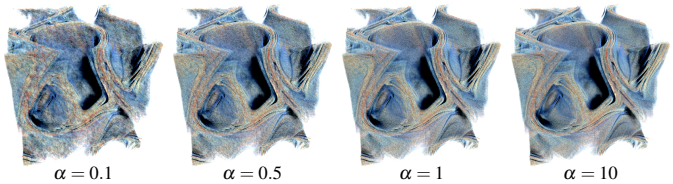

Fig. 1: Results for different choices of the energy weight α. We follow Lehtinen et al. [3] and select $\alpha = 1$ in all examples in the paper. The above images show early results after only 20 Monte Carlo iterations of our joint ratio-Fourier tracking with gradient domain rendering.

2 Convergence

Fig. 3, shows the results of 80 iterations in the Mixer data set for delta tracking (D), gradient domain (G), gradient with ratio (GR), gradient with ratio-Fourier (GRF) or only Fourier (GF). We list the computation time, the root-mean-square error (RMSE) and the structural similarity index (SSIM) when comparing to a ground truth image. Introducing gradient domain considerably improves the noise reduction, while our transmittance approximations speed up the computation, resulting in smooth and visually noise free images after far less iterations. In order to match the same error quality of this example, the Günther et al. [1] approach needs at least 1100 iterations. Thus, rendering a 80 frames animation with this technique would escalate to a computation time of 79 hours, instead of the 10 hours that our gradient-Fourier approach needs. Similar behavior for the Mixer and Asteroid data sets can be seen in Fig. 2, where the convergence after 80 iterations (Fig. 8 of main paper) can be seen with time (*sec*) in the x-axis.

3 Approximation Artifacts

In difficult lighting situations, such as the example shown in Fig. 6 top for the Asteroid data set, the Fourier approximation of the transmittance underestimates certain problematic areas, resulting in apparent darkened areas. These extreme situation, where the smooth approximation could not retain the sudden changes in illumination inside the corridor, can be completely avoided by the ratio-Fourier approach, that detects the high difference between the approximation and the computed transmittance and does not switch to Fourier. Insufficient Fourier signal approximation can cause ringing artifacts, as the example shown in Fig. 6 middle for the Wall-Mounted Cylinder data set. In the last row of Fig. 6, we show that using a lower resolution can eliminate this artifact (bottom middle), since the transmittance is then also smoothed but undetectable for our eyes. However, using too low resolutions (bottom right) leads to a darker image due to a poor illumination approximation.

- *Irene Baeza Rojo and Tobias Günther are with the Computer Graphics Laboratory, ETH Zürich. E-mail: irene.baeza|tobias.guenther@inf.ethz.ch.*
- *Markus Gross is head of the Computer Graphics Laboratory, ETH Zürich. E-mail: grossm@inf.ethz.ch.*

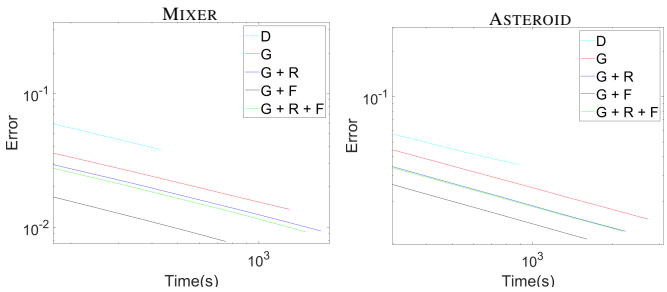

Fig. 2: Logarithmic convergence plot of the Mixer and Asteroid data sets data set showing error in x-axis and time (*sec*) in y-axis.

4 Error Tolerance

In Fig. 7 of the main paper, we used the ECMWF flow to study the error tolerance ε of our joint ratio-Fourier transmittance estimator in comparison with the ratio-tracking estimator [4] and a purely Fourier approximation approach. Fig. 5 shows a close up of these images, where artifacts due to the approximations are clearly visible when comparing with the ratio-tracking reference solution in 5a.

5 Fourier Maps Resolution

Fig. 4 shows the results obtained using different map resolutions in the ECMWF data set after 100 iterations. The pre-computation of the maps is done once in a preprocess and is in the order of seconds, as indicated in caption of each configuration. We found that a resolution of around 500×500 pixels for the Fourier maps (4c) is sufficient for all examples. The impact of incrementing the resolution further is very small and not visually perceptible, since now most of the approximation error is due to the low number of Fourier coefficients that fail to capture high frequency transmittance details.

6 High Resolution comparisons

Figs. 7, 8 and 9 show high resolution examples using gradient domain with ratio tracking [4] (GR), gradient domain with ratio-Fourier (GRF) and gradient domain with Fourier (GF).

References

[1] T. Günther, A. Kuhn, and H. Theisel. MCFTLE: Monte Carlo rendering of finite-time Lyapunov exponent fields. *Computer Graphics Forum (Proc. EuroVis)*, 35(3):381–390, 2016.

[2] G. Haller. Distinguished material surfaces and coherent structures in three-dimensional fluid flows. *Physica D: Nonlinear Phenomena*, 149(4):248–277, Mar. 2001.

[3] J. Lehtinen, T. Karras, S. Laine, M. Aittala, F. Durand, and T. Aila. Gradient-domain metropolis light transport. *ACM Trans. Graph.*, 32(4):95:1–95:12, July 2013.

[4] J. Novák, A. Selle, and W. Jarosz. Residual ratio tracking for estimating attenuation in participating media. *ACM Transaction on Graphics (SIGGRAPH Asia)*, 33(6):179:1–179:11, 2014.

[5] E. Woodcock, T. Murphy, P. Hemmings, and S. Longworth. Techniques used in the GEM code for Monte Carlo neutronics calculations in reactors and other systems of complex geometry. In *Proc. Conf. Applications of Computing Methods to Reactor Problems*, volume 557. Argonne National Laboratory, 1965.

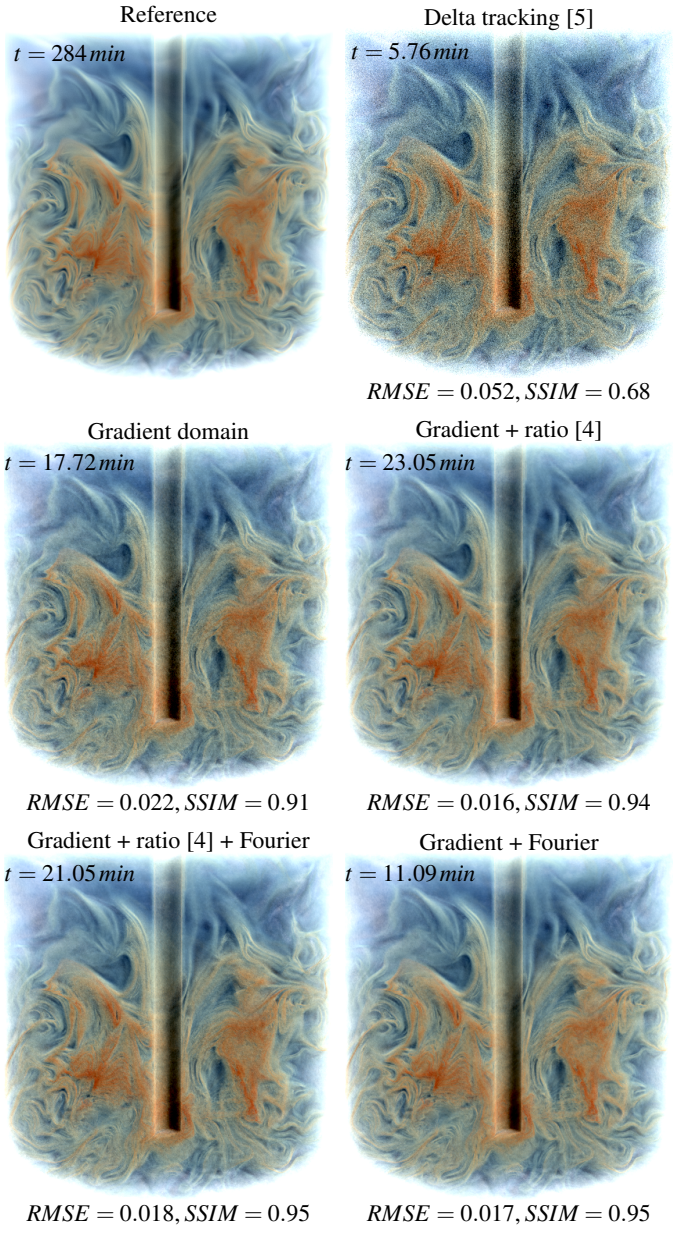

Fig. 3: Comparison of techniques in the MIXER data set after 80 iterations for 500×500 images. We list the time (t) in *min*, the root-mean-square error (RMSE) and the structural similarity index (SSIM). Although the use of gradient domain increments the time per iteration, the noise for the previous approach [1] is still very noticeable, while our methods already show indistinguishable images compared to the reference.

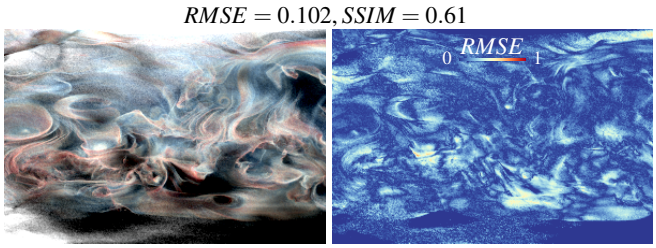

(a) 50×50 Fourier map, $t = 0.08\,s$.

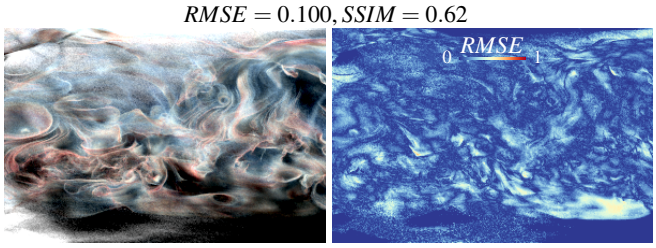

(b) 100×100 Fourier map, $t = 0.25\,s$.

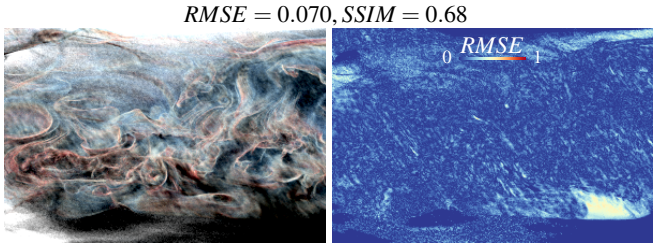

(c) 500×500 Fourier map, $t = 12.12\,s$.

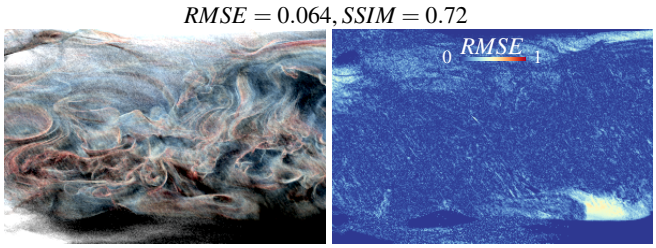

(d) 1000×1000 Fourier map, $t = 20.59\,s$.

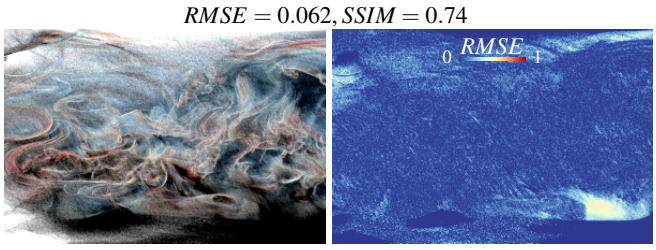

(e) 1500×1500 Fourier map, $t = 25.31\,s$.

Fig. 4: Comparison of different Fourier map resolutions in the ECMWF dataset after 100 iterations using gradient domain with Fourier approximation of transmittance. From resolutions of 500×500 and higher, the improvements in the transmittance estimation are very subtle.

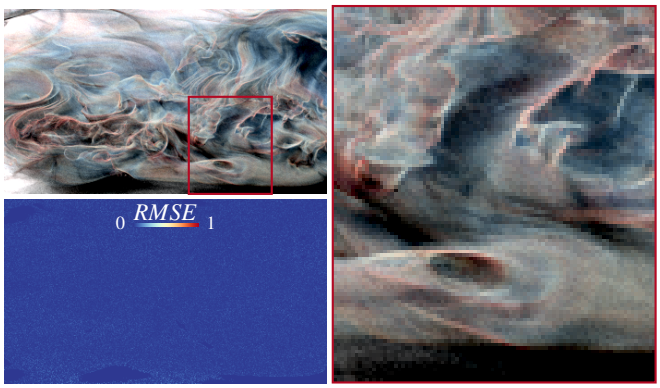

(a) Ratio-tracking, $RMSE = 0.018, SSIM = 0.93$.

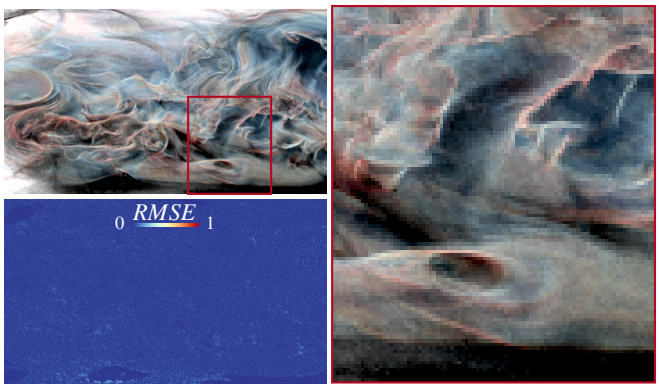

(b) Ratio-Fourier with $\varepsilon = \bar{\sigma}_t/100$, $RMSE = 0.020, SSIM = 0.91$.

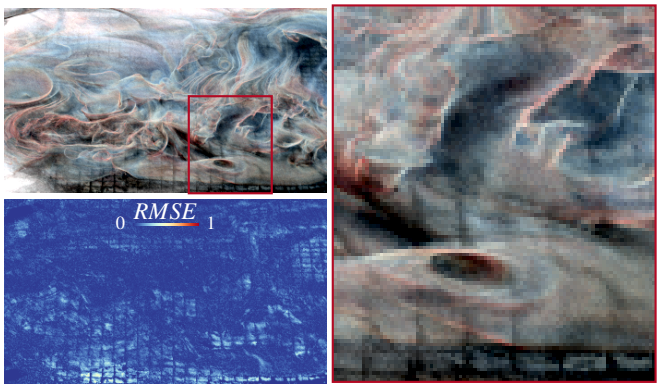

(c) Ratio-Fourier with $\varepsilon = \bar{\sigma}_t/10$, $RMSE = 0.046, SSIM = 0.82$.

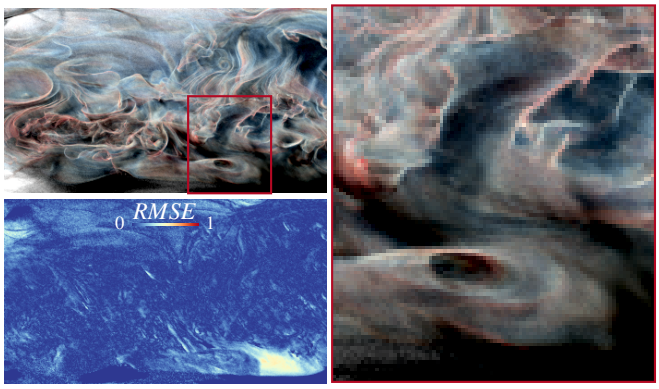

(d) Fourier approximation, $RMSE = 0.064, SSIM = 0.80$.

Fig. 5: Detailed zooms and error from Fig.7 of the main paper comparing our joint ratio-Fourier transmittance estimator with ratio tracking [4] and our pure Fourier approximation of the transmittance.

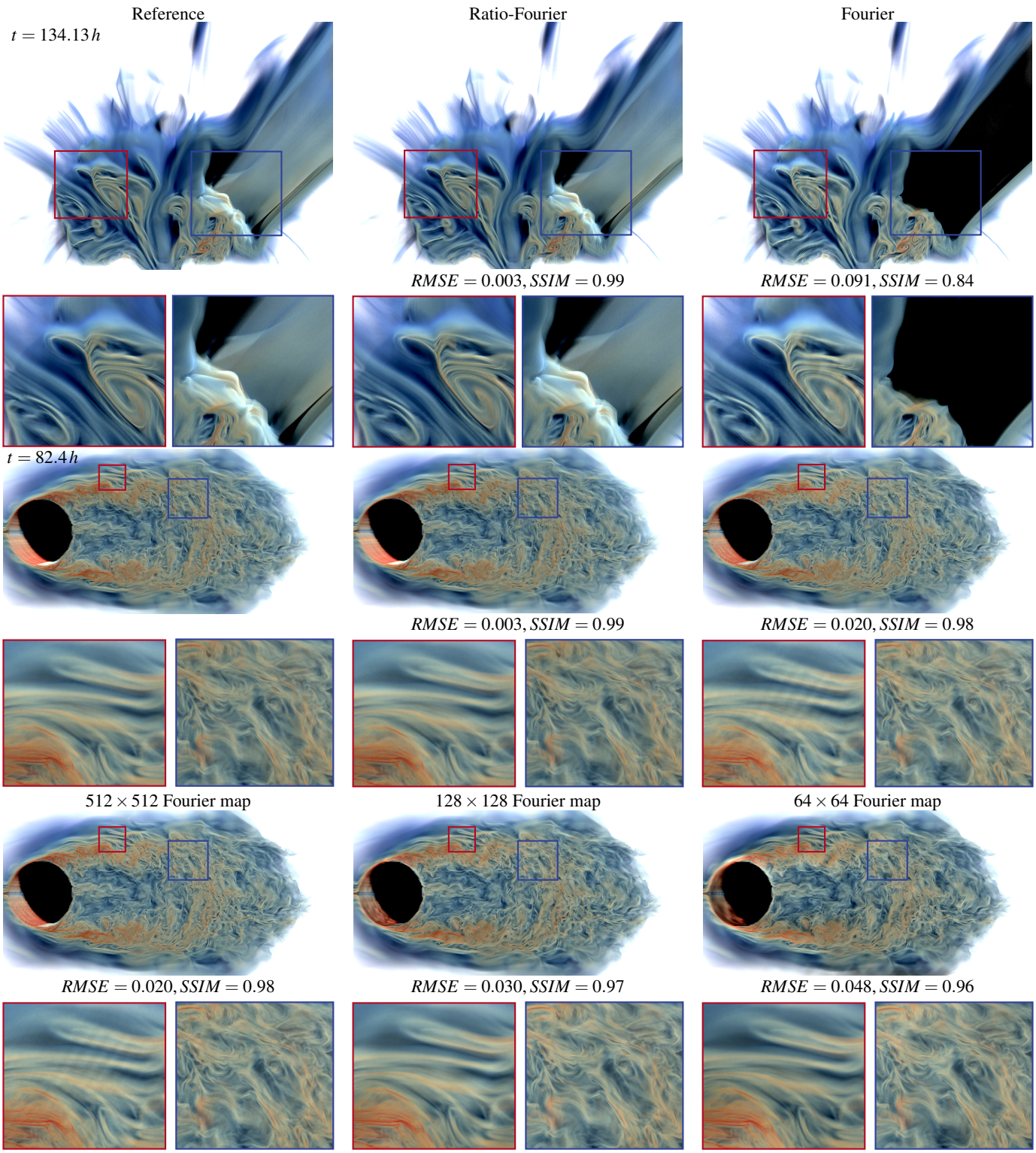

Fig. 6: Comparison of artifacts in ratio-Fourier and Fourier only transmittance approximation with a ground truth image computed with $1k$ iterations of gradient domain. In the ASTEROID (top), the illumination of the entry corridor of the asteroid is completely underestimated by the Fourier approximation, while the ratio-Fourier approach avoids the artifact by never switching to Fourier transmittance through that area. In the WALL-MOUNTED CYLINDER (middle and bottom), using a high resolution Fourier map creates ringing artifacts that can be avoided by using lower resolutions that smooth the transmittance or switching to a ratio-Fourier approach.

ASTEROID

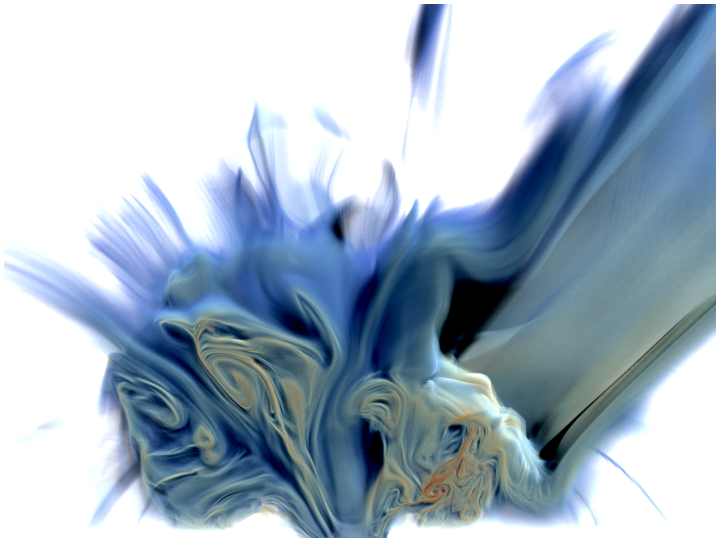

MIXER

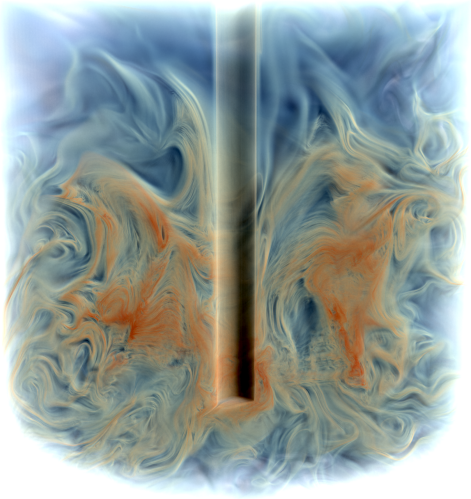

ECMWF

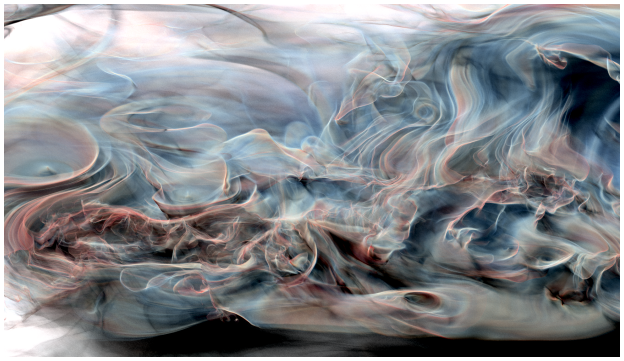

WALL-MOUNTED CYLINDER

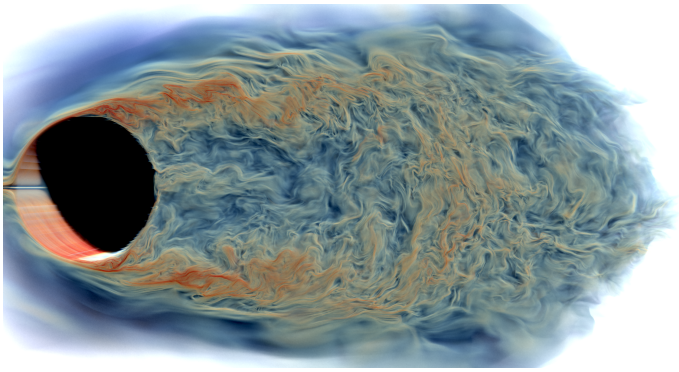

CTBL

Fig. 7: High resolution images computed using gradient domain with ratio tracking (GR) for the ASTEROID (1920×1440), MIXER (2000×2000), ECMWF (1960×1120), WALL-MOUNTED CYLINDER (2400×1200) and the CTBL (900×480) data sets.

ASTEROID

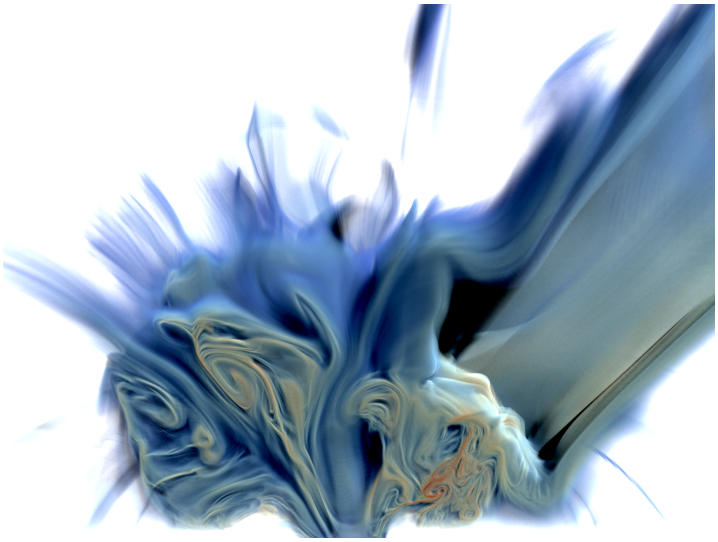

MIXER

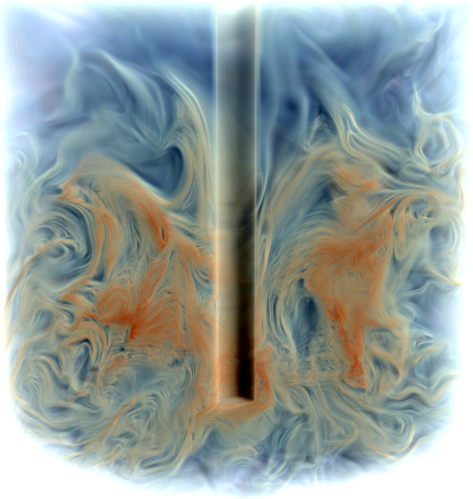

ECMWF

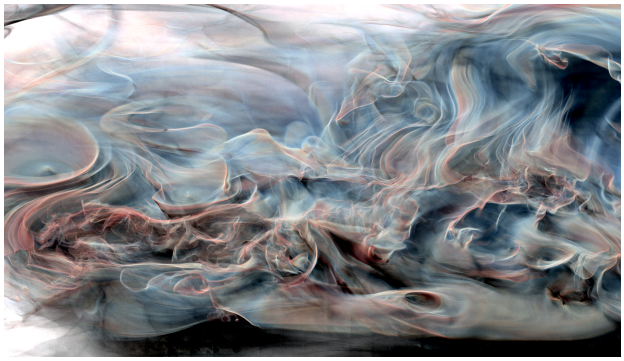

WALL-MOUNTED CYLINDER

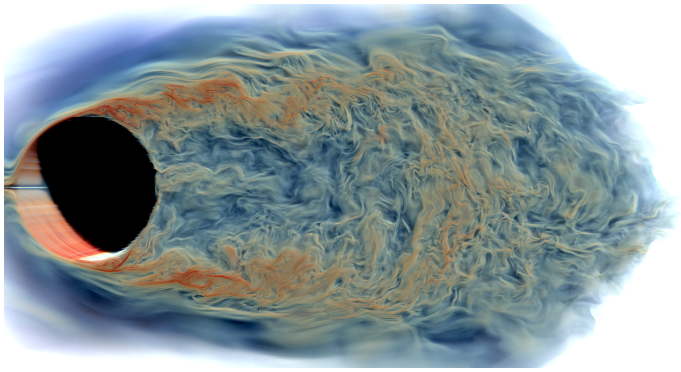

CTBL

Fig. 8: High resolution images computed using gradient domain with ratio-Fourier (GRF) for the ASTEROID (1920×1440), MIXER (2000×2000), ECMWF (1960×1120), WALL-MOUNTED CYLINDER (2400×1200) and the CTBL (900×480) data sets.

ASTEROID

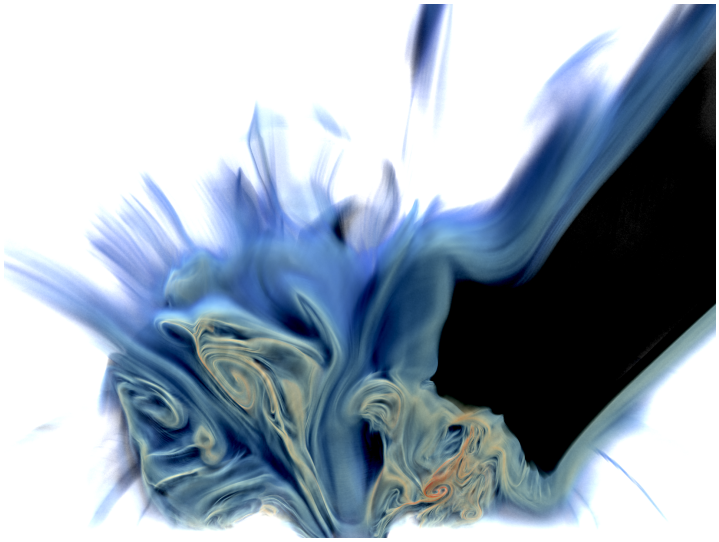

MIXER

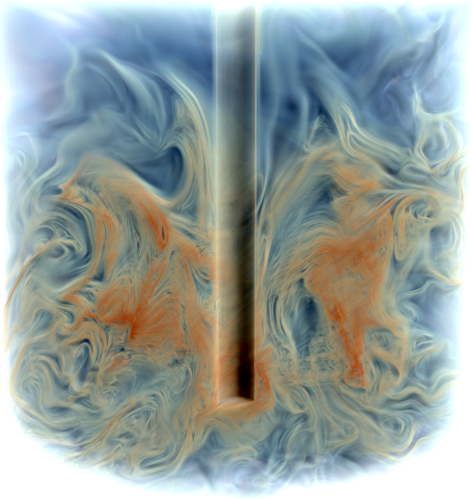

ECMWF

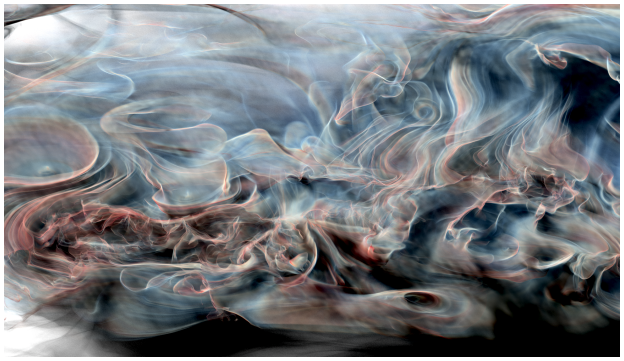

WALL-MOUNTED CYLINDER

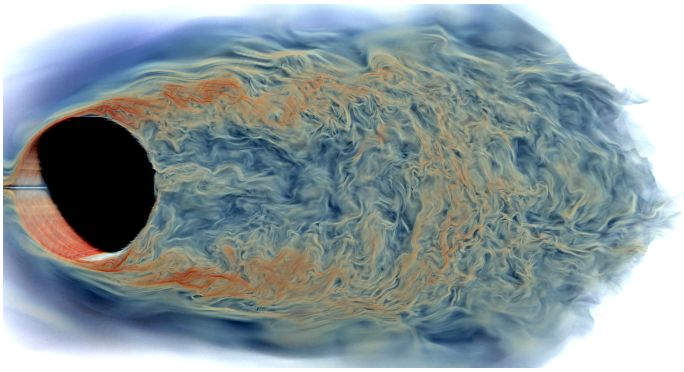

CTBL

Fig. 9: High resolution images computed using gradient domain with Fourier (GF) for the ASTEROID (1920×1440), MIXER (2000×2000), ECMWF (1960×1120), WALL-MOUNTED CYLINDER (2400×1200) and the CTBL (900×480) data sets.